

A closed-form solution for a fluid-structure system: shear beam-compressible fluid

Amirhossein Keivani^{*1}, Ahmad Shooshtari² and Ahmad Aftabi Sani³

^{1,2} Civil Engineering Faculty, Ferdowsi University of Mashhad, Mashhad, Iran

³ Department of Civil Engineering, Mashhad Branch, Islamic Azad University, Mashhad, Iran

(Received February 5, 2013, Revised March 20, 2013, Accepted March 29, 2013)

Abstract. A closed-form solution for a fluid-structure system is presented in this article. The closed-form is used to evaluate the finite element method results through a numeric example with consideration of high frequencies of excitation. In the example, the structure is modeled as a cantilever beam with rectangular cross-section including only shear deformation and the reservoir is assumed semi-infinite rectangular filled with compressible fluid. It is observed that finite element results deviate from the closed-form in relatively higher frequencies which is the case for the near field earthquakes.

Keywords: fluid-structure interaction; closed-form solution; shear beam; hydrodynamic pressure

1. Introduction

Most of physical problems in engineering can be expressed by a boundary value problem (BVP). Fluid-structure interaction is one of these problems which have been the subject of many researches for decades. There exist numerical methods as well as analytical approaches for the solution of the corresponding BVP. However, due to complexity of the mentioned problem, a few numbers of analytical solutions to several especial cases are available in contrast to the numerical ones. Also, in many cases, simplifications have to be imposed to the original BVP assumptions to achieve an analytical solution.

The first analytical solution considering the effect of incompressible fluid on a rigid dam for horizontal excitation was introduced by Westergaard (1933). He proposed the concept of added mass as an alternative for dynamic analysis of dams. Brahtz and Heilborn (1933) studied the effect of compressibility of fluid as well as flexibility of structure using an iterative process. They assumed a linear deformed shape for the dam which accounted for both shear and flexural deformation. However, their assumption of a linear deformed shape was a relatively good approximation for only the first fundamental frequency. Analytical expression for hydrodynamic pressure on gravity dams under the assumption of invariant fundamental flexural modes for deformation was proposed by Chopra (1967), where shear deformations were ignored.

Nath (1971) implemented the finite difference method together with analytical expressions to

*Corresponding author, Ph.D. Candidate, Email: amir.keivani@gmail.com

solve the coupled water-dam equations of motion. In his work, the structure was assumed a cantilever Timoshenko beam considering both shear and bending deflections with viscous damping. The radiation damping of the reservoir was neglected under finite reservoir assumption. Similarly, an analytic-numeric method was proposed by Liam Finn and Varoglu (1973). They used Laplace transformation to find an analytical expression for hydrodynamic pressures on dams. In their model, the reservoir was infinite and the pressure term, as an external load, was a function of wet surface deflections. They used finite elements to approximate the deflection function. Their results were in good agreement with conventional finite element method. Chakrabarti and Chopra (1972) offered a frequency response function for vertical excitation of gravity dams with infinite reservoir. The deformation of the dam was approximated by its first fundamental mode shape.

Saini *et al.* (1978) used finite element combined with infinite fluid elements for evaluation of coupled response of gravity dams. They concluded that the radiation damping must be considered for high frequencies of excitation. After that, Chwang (1978) derived a closed-form solution for distribution of hydrodynamic pressure on rigid dams with constant sloping of wet surface. In his study, incompressible fluid and constant horizontal excitation were considered. Chopra and Chakrabarti (1981) incorporated water-dam-foundation interaction into their finite element analysis and approximated the dam deformation by combination of Ritz vectors. Both vertical and horizontal excitations were considered. Humar and Raufaiel (1983) suggested a radiation boundary condition for finite element analysis. It was applied to several rigid dams with vertical and sloping faces and was concluded that the proposed method covers wider range of excitation frequencies in comparison with Sharan radiation damping. Their results indicated that inclination in the wet surface of the dam reduces hydrodynamic pressures. Natural frequencies of a fill dam with a wedge section was calculated by Kishi *et al.* (1987) considering both shear and bending effects. They implemented finite difference in their calculations. The shearing behavior was found to be dominating in their work.

Tsai and Lee (1990) determined the hydrodynamic pressure on dams using a semi-analytical procedure. An arbitrary slope could be assumed for upstream face of dam and compressibility of water was taken into account. However, the flexibility of dam was neglected in his work. Sharan (1992) proposed a radiation boundary condition in terms of a series, enabling the application of energy dissipation at reservoir bottom in near field. The proposed boundary condition was independent from dam-near field characteristics and was implemented for arbitrary shape of upstream dam face. However, the dam body and the near field required to be modeled numerically. Ghobara *et al.* (1994) developed a simplified method for analysis of gravity dams considering the monolith-contraction joint interaction. They simplified the problem using vertical beam elements for the monolith with constant cross section. The monoliths were connected longitudinally by shear links. Moreover, Tsai *et al.* (1992) adopted the exact transmitting boundary condition for time domain. They utilized boundary element method for near field part of reservoir to comply with its complex geometry. Aviles and Li (1998) suggested a method for evaluation of hydrodynamic pressures on non-vertical rigid dams including viscosity and compressibility of fluid. They used Trefftz functions and minimized the error function only on the dam-water interface to increase accuracy. Nasserzare *et al.* (2000) approximated the natural frequency of arch dams utilizing a cantilever beam. Only flexural deformation was taken into account and mode shapes of the beam were applied in the interaction boundary condition. Attarnejad and Farsad (2005) presented a closed form solution for dam-reservoir interaction considering a flexural beam with variable cross section of the dam. They assumed infinite reflective reservoir and used modal decomposition in their solution.

A closed-form formulation was presented by Bouannani and Proulx (2003) for evaluation of hydrodynamic pressures on rigid dams in frequency domain. The formulation included the effect of damping due to reservoir bottom together with infinite reservoir assumption. The effect of ice covering of reservoir was investigated by Bouannani and Paultre (2005) using boundary element method. They also studied the effect of several reservoir far field boundary conditions including an analytical radiation boundary condition. Furthermore, some recent studies have studied the hydrodynamic effects on gravity dams using analytical approach which are not discussed here for the sake of brevity (Bejar 2010, Bouaanani and Miquel 2010, Bouaanani and Perrault 2010, Miquel and Bouaanani 2010).

The aim of this paper is to solve the BVP of fluid-structure system by providing a closed-form solution. Moreover, closed-form results are used to evaluate the accuracy of the finite element method especially for higher frequencies of excitation. Special attention is devoted to shear deformation of the structure.

The first section of this paper is concerned with definition of the governing differential equations of fluid-structure system and the corresponding boundary conditions. Subsequent sections deal with presentation of closed-form and finite element solutions. Results of a numerical example are thoroughly compared, to investigate the accuracy of each method as well as the effective parameters.

2. Definition of governing BVP

Any boundary value problem consists of one or more differential equations and related boundary conditions (BC). In this study, the fluid-structure system consists of two differential equations regarding the fluid and the structure. Each domain includes independent boundary conditions and one dependent boundary condition, usually referred to as interaction boundary condition. In the following, initially, the fluid differential equation and its independent BCs. are introduced. Additionally, the structure differential equation and its independent BCs. will be presented. Finally, the interaction BC. will be explained and incorporated into the solution.

2.1 Fluid governing equations

Assuming irrotational flow, small amplitude of motion and inviscid fluid, the differential equation of the fluid can be derived from the well known Navier-Stokes equation. The resultant equation is referred to as wave equation and is given by

$$\frac{\partial^2 P}{\partial x^2} + \frac{\partial^2 P}{\partial y^2} = \frac{1}{c^2} \frac{\partial^2 P}{\partial t^2} \quad (1)$$

where, c is the wave propagation speed and P is unknown pressure. Apparently, in Eq. (1), pressure is a function of coordinates and time. This equation reduces to Laplace equation, for incompressible fluid which wave propagation speed is assumed infinity. Alternatively, one may solve Eq. (1) in frequency domain. In this case, the following transformation is applied

$$P(x, y, t) = P^*(x, y, \omega) e^{i\omega t} \quad (2)$$

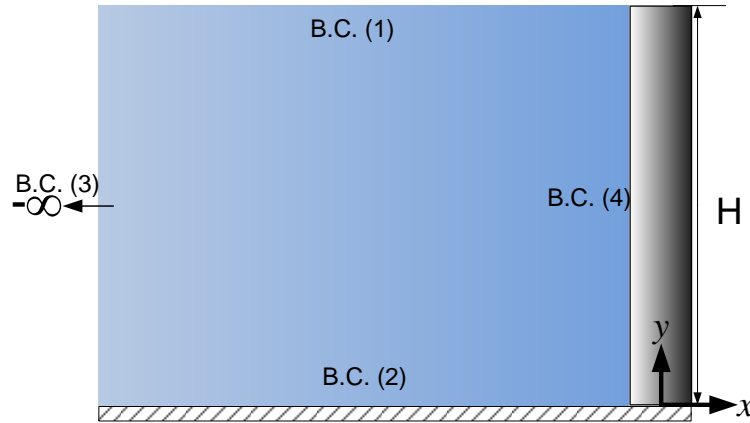


Fig. 1 Fluid-structure system

where, ω is the excitation frequency and P^* denotes pressure in frequency domain. Consequently, the resulting fluid-domain equation is written as

$$\frac{\partial^2 P^*}{\partial x^2} + \frac{\partial^2 P^*}{\partial y^2} + \frac{\omega^2}{c^2} P^* = 0 \quad (3)$$

For simplicity, P^* will be denoted by P , hereafter. Likewise, all boundary conditions are transferred to frequency domain by a similar transformation. These boundary conditions include both the specified values of pressure on one side and the flux of the pressure function on the other sides, as numbered in Fig. 1.

The fluid is assumed to have no surface waves. This enforces the relative pressure (P) to be zero at the surface resulting in the first boundary

$$P(x, H, \omega) = 0 \quad (4)$$

In addition, it can be shown that the flux of the pressure in fluid is equal to negative normal acceleration of the boundary multiplied by the fluid mass density. As a result, since only the horizontal excitation is considered, the values of normal accelerations on the second boundary are zero

$$\left. \frac{\partial P}{\partial (-y)} \right|_{(x,0,\omega)} = 0 \quad (5)$$

The third BC is related to the infinite part of fluid region and is defined by

$$\lim_{x \rightarrow -\infty} P(x, y, \omega) = 0 \quad (6)$$

which states that the hydrodynamic pressure of fluid vanishes in long distances from the excitation center. The last boundary condition of the fluid region is the interaction boundary condition. Since this is a dependent boundary condition and requires the introduction of governing equations of the

structure, it will be discussed in the subsequent sections.

2.2 Structure governing equations

In this study, the structure is considered as a vertical shear beam with uniform rectangular cross-section. Also, mass and shear stiffness are constantly distributed along the beam height. For the case of a gravity dam with considerable transverse thickness, shearing deformations are more significant. Therefore, only shear deformations are considered. Moreover, ignoring rotational inertia and considering small amplitude of motion, one can derive the beam equation of motion in the form of

$$GA \frac{\partial^2 u}{\partial y^2} = \rho \frac{\partial^2 u_T}{\partial t^2} \quad (7)$$

where, GA , ρ and u are constant shear rigidity, mass density and relative displacement of the beam, respectively. Also, u_T is the total displacements of the beam (including the base displacements). This equation can be transferred into the frequency domain employing the following transformations

$$\begin{cases} u(x, t) = u^*(x, \omega) e^{i\omega t} \\ u_g(x, \omega) = 1 e^{i\omega t} \end{cases} \quad (8)$$

In the above relations, u^* and u_g represent relative and absolute ground displacement in the frequency domain, respectively. In addition, ω is the frequency of excitation. Thus, incorporating these transformations into Eq. (7) yields

$$GA \frac{\partial^2 u^*}{\partial y^2} = -\rho \omega^2 (u^* + 1) \quad (9)$$

It should be noted that the above equation is written regardless of hydrodynamic pressure. However, the beam in Fig. 1 is adjacent to the fluid which exerts a distributed hydrodynamic pressure on the beam as shown in Fig. 2. Also, for simplicity in writing, u^* will be replaced with u .

As a result, Eq. (9) should be corrected by adding the hydrodynamic load into the right side

$$GA \frac{\partial^2 u}{\partial y^2} = -\rho \omega^2 (u + 1) - P|_{(0, y, \omega)} \quad (10)$$

The related boundary conditions should be expressed in frequency domain. The first boundary condition is the zero displacement at the base of the beam ($y = 0$)

$$u(0, \omega) = 0 \quad (11)$$

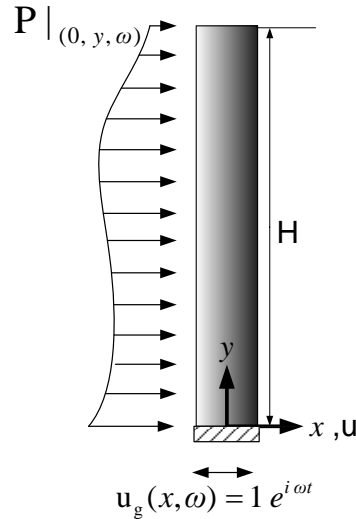


Fig. 2 The pressure of fluid on the structure as an external loading

and the zero shear stress at free end of the beam ($y = H$) yields

$$\mathbf{G} \frac{\partial \mathbf{u}}{\partial y} \Big|_{(H, \omega)} = 0 \quad (12)$$

Having introduced two boundary conditions for the structure, only interaction boundary condition remains unknown and is explained in the next section.

2.3 Interaction boundary condition

The interaction boundary condition defines a relation between the fluid and the structure; the normal acceleration on the wet surface is equal to total acceleration of the adjacent structure, due to vertical face of the beam. Therefore, since the outward normal vector of fluid region is in positive x direction, the interaction boundary condition can be written as

$$\frac{\partial P}{\partial x} \Big|_{(0, y, t)} = -\rho_F \left(\frac{\partial^2 \mathbf{u}_T}{\partial t^2} \right) \quad (13)$$

Likewise, we apply the frequency domain transformation to the above equation. The result together with the equations of motion and corresponding boundary conditions is summarized below. In fact, the following table forms the corresponding BVP.

3. Closed-form solution of the fluid-structure system

To solve the mentioned boundary value problem, alternatively, one may apply separation of

variable technique. The first equation to be solved is the fluid governing equation (Eq. (3)). This equation is homogenous, thus by introducing $P = XY$, where $X(x)$ and $Y(y)$ are single variable functions, Eq. (3) reduces to

$$\frac{X''}{X} + \frac{\omega^2}{c^2} = -\frac{Y''}{Y} \tag{14}$$

Since the right and left sides of the above equation are functions with different variables, they both should equal to a constant value. Therefore, assuming both sides equal to the unknown constant λ^2 results in

$$\begin{cases} \frac{X''}{X} + \frac{\omega^2}{c^2} = \lambda^2 \\ \frac{Y''}{Y} = -\lambda^2 \end{cases} \Rightarrow \begin{cases} X'' - \left(\lambda^2 - \frac{\omega^2}{c^2}\right)X = 0 \\ Y'' + \lambda^2 Y = 0 \end{cases} \tag{15}$$

The solutions of these equations are

$$\begin{cases} X(x) = A e^{-kx} + B e^{kx} \\ Y(y) = A' \sin(\lambda y) + B' \cos(\lambda y) \end{cases} \tag{16}$$

where, A, B, A' and B' are constants and $k^2 = \lambda^2 - \frac{\omega^2}{c^2}$. The three of these constants which satisfy the first three boundary conditions of the fluid domain may directly be calculated

$$\begin{cases} \lim_{x \rightarrow -\infty} P(x, y, \omega) = 0 \Rightarrow A = 0 \\ \left. \frac{\partial P}{\partial y} \right|_{(x,0,\omega)} = 0 \equiv Y'(0) = 0 \Rightarrow A' = 0 \\ P(x, H, \omega) = 0 \equiv Y(H) = 0 \Rightarrow B' \neq 0 \ \& \ \lambda_j = \frac{(2j-1)}{2H} \pi : j = 1, 2, \dots \end{cases} \tag{17}$$

Substituting these constants into Eq. (16) and forming pressure function, the pressure can be written in the form of an infinite series

$$P(x, y, \omega) = \sum_{j=1}^{\infty} B_j e^{k_j x} \cos(\lambda_j y) \tag{18}$$

To evaluate the last constant B_j , the interaction boundary condition is employed. Therefore, using Eqs. (13) and (18) at $x = 0$ we have

$$\sum_{j=1}^{\infty} B_j k_j \cos(\lambda_j y) = \rho_F \omega^2 (u + 1) \tag{18}$$

Table 1 Governing equations and boundary conditions of the problem.

	Fluid	Structure
Unknown function	$P(x, y, \omega)$	$u(y, \omega)$
Governing differential equation	$\frac{\partial^2 P}{\partial x^2} + \frac{\partial^2 P}{\partial y^2} + \frac{\omega^2}{c^2} P = 0$	$GA \frac{\partial^2 u}{\partial y^2} + \rho \omega^2 u = -\rho \omega^2 - P _{(0, y, \omega)}$
Boundary conditions	$P(x, H, \omega) = 0$	$u(0, \omega) = 0$
	$\left. \frac{\partial P}{\partial y} \right _{(x, 0, \omega)} = 0$	
	$\lim_{x \rightarrow -\infty} P(x, y, t) = 0$	$\left. \frac{\partial u}{\partial y} \right _{(H, \omega)} = 0$
	$\left. \frac{\partial P}{\partial x} \right _{(0, y, \omega)} = \rho_F \omega^2 (u + 1)$	

However, calculation of constants are B_j requires determination of unknown values of displacement function. Thus, the displacement function (u) should be obtained by solving Eq. (10). In order to solve Eq. (10), the pressure term in the right side of the equation is replaced by Eq. (18) at $x=0$

$$GAu' + \rho \omega^2 u = -\rho \omega^2 + \sum_{j=1}^{\infty} B_j \cos(\lambda_j y) \quad (20)$$

This equation is a second order non-homogenous differential equation which includes two types of particular solutions together complimentary solution. The complimentary solution of the homogenous form can be easily calculated by

$$\begin{cases} \alpha = \sqrt{\frac{\rho \omega^2}{GA}} \Rightarrow u'' + \alpha^2 u = 0 \\ u_c = c_1 \cos(\alpha y) + c_2 \sin(\alpha y) \end{cases} \quad (21)$$

where, c_1 and c_2 are constant that can be obtained from boundary conditions subsequent to determination of particular solution. Meanwhile, the first particular solution regarding the first term in the right side of Eq. (20) is

$$GAu'' + \rho \omega^2 u = -\rho \omega^2 \Rightarrow u_{p1} = -1 \quad (22)$$

Moreover, the second term in the right side of Eq. (20) includes a summation of similar cosine functions. Therefore, one may solve the following equation to obtain the general form of the particular solution

$$GA u_j'' + \rho \omega^2 u_j = B_j \cos(\lambda_j y) \quad (23)$$

The solution of the above equation has the form of

$$u_j = D_j \cos(\lambda_j y) \quad (24)$$

In which D_j is an unknown constant and is determined by substituting Eq. (24) into Eq. (23)

$$D_j = \frac{\alpha^2 B_j}{\rho \omega^2 (\alpha^2 - \lambda_j^2)} \quad (25)$$

Finally, the general solution of Eq. (20) can be expressed as

$$u(y) = c_1 \cos(\alpha y) + c_2 \sin(\alpha y) - 1 + \sum_{j=1}^{\infty} D_j \cos(\lambda_j y) \quad (26)$$

Thereafter, boundary conditions should be applied to evaluate the unknown constants c_1 and c_2 . Beforehand, it is convenient to define some parameters

$$\begin{cases} \beta = \tan(\alpha H) \\ \gamma = \frac{1}{\alpha \cos(\alpha H)} \end{cases} \quad (27)$$

Also, additional parameters related to j-counter are introduced

$$\begin{cases} \sigma_j = \frac{1}{GA(\alpha^2 - \lambda_j^2)} \\ \delta_j = [\lambda_j (-1)^{j+1} \gamma - \beta] \sigma_j \end{cases} \quad (28)$$

Applying boundary conditions introduced in Eqs. (11) and (12), the constants c_1 and c_2 will be

$$\begin{cases} c_1 = 1 - \sum_{j=1}^{\infty} \sigma_j B_j \\ c_2 = \beta + \sum_{j=1}^{\infty} \delta_j B_j \end{cases} \quad (29)$$

Replacing (29) and (28) into Eq. (26) results in

$$u(y) = \left(1 - \sum_{j=1}^{\infty} \sigma_j B_j\right) \cos(\alpha y) + \left(\beta + \sum_{j=1}^{\infty} \delta_j B_j\right) \sin(\alpha y) - 1 + \sum_{j=1}^{\infty} \sigma_j B_j \cos(\lambda_j y) \quad (30)$$

In the above equation, the only unknown coefficients are B_j . In order to determine these coefficients, interaction boundary condition denoted by Eq. (19) should be applied. Moreover, since both sides of Eq. (19) contain B_j , a novel technique is employed to extract these unknowns. In this technique, both sides are multiplied by $\cos(\lambda_i y)$ and integrated along the beam height

$$B_i k_i \frac{H}{2} = \rho_F \omega^2 \int_0^H [u(y) + 1] \cos(\lambda_i y) dy \quad (31)$$

The left side of Eq. (31) is reduced to a simple form due to orthogonal property of cosine functions. However, the coefficients of B_j , which exist in the definition of $u(y)$ in the right side, are unknown and need to be determined through integration. In the integration process, two integrals are encountered which their closed-forms exist and are expressed by

$$\begin{aligned} I_1^i &= \int_0^H \sin(\alpha y) \cos(\lambda_i y) dy = \frac{2H[2\alpha H - (1-2i)\pi(-1)^i \sin(\alpha H)]}{(2\alpha H)^2 - (1-2i)^2 \pi^2} \\ I_2^i &= \int_0^H \cos(\alpha y) \cos(\lambda_i y) dy = \frac{H \cos(i\pi - \alpha H)}{2\alpha H + (1-2i)\pi} - \frac{H \cos(i\pi + \alpha H)}{2\alpha H - (1-2i)\pi} \end{aligned} \quad (32)$$

Replacing I_1^i and I_2^i in Eq. (31) and using several auxiliary variables introduced in Eq. (32) results in a system of equations which B_j can be calculated from

$$\left. \begin{aligned} a_{ij} &= \delta_j I_1^i - \sigma_j I_2^i \\ d_i &= \frac{H}{2} \left(\frac{k_i}{\rho_F \omega^2} + \sigma_i \right) \\ b_i &= -I_2^i - \beta I_1^i \end{aligned} \right\} \Rightarrow d_i B_i + \sum_{j=1}^{\infty} a_{ij} B_j = b_i \quad (33)$$

Although this system of equations comprise infinite terms, it can be shown that considering limited number of terms provides relatively accurate results. Alternatively, one may use more terms of series to achieve desired accuracy.

4. Finite element method

According to widespread implementation of the finite element method, the methodology and corresponding numerical model are briefly presented in this section.

In the finite element method, a discretization is made over the continuous unknown function of the governing differential equations by dividing a region into sub-regions referred to as *elements*. This results in a system of linear equations in which the responses are values of the unknown function in finite number of points referred to as *nodes*. Also, in order to evaluate the function value of an arbitrary point in the region, shape functions are employed as means of interpolation.

For this study, the types of elements used are:

1-Shear-beam element with one translational degree of freedom at each end.

2-Four-node fluid element with one pressure degree of freedom per node.

3-Fluid hyper-element with two nodes in each sub-layer.

Accordingly, shear-beam elements are used to model a cantilever beam. The stiffness and mass matrices of the beam element are

$$\mathbf{K} = \frac{GA}{L} \begin{bmatrix} 1 & -1 \\ -1 & 1 \end{bmatrix}, \mathbf{M} = \frac{1}{6} \rho L \begin{bmatrix} 2 & 1 \\ 1 & 2 \end{bmatrix} \quad (34)$$

where ρ is beam mass density and L denotes the length of each element.

The fluid domain adjacent to the beam (near field) and the infinite fluid domain (far field) are modeled by square and hyper-elements, respectively.

A typical finite element model is shown in Fig. 3. In addition, since the accuracy of response relies on the number of elements, different meshes are investigated in this study. However, a 10×10 mesh for the near field reservoir and ten elements for the beam and the hyper-element provide sufficient accuracy.

The corresponding finite element matrix equation of fluid-structure system for horizontal excitation may be defined by the following equation in frequency domain (Lotfi 2004)

$$\left[\begin{array}{c|c} \mathbf{K} - \omega^2 \mathbf{M} & -\mathbf{B}^T \\ \hline -\rho_F \omega^2 \mathbf{B} & \mathbf{H} + \mathbf{H}_h - (\omega^2 / c^2) \mathbf{G} \end{array} \right] \begin{pmatrix} \mathbf{U} \\ \mathbf{P} \end{pmatrix} = \begin{pmatrix} -\mathbf{M} \mathbf{J} \mathbf{a}_g \\ -\rho_F \mathbf{B} \mathbf{J} \mathbf{a}_g \end{pmatrix} \quad (35)$$

where, \mathbf{K}, \mathbf{M} are stiffness and mass matrices of the structure and \mathbf{H}, \mathbf{G} represent corresponding matrices of the fluid domain. \mathbf{H}_h is hyper-element contribution part in the far field and \mathbf{B} is the interaction matrix. Also, $\mathbf{J} \mathbf{a}_g$ is the excitation vector. The finite element matrices of the fluid domain are presented in the Appendix.

The beam displacements and the fluid pressures are obtained by solving Eq. (35) for any specified excitation frequency.

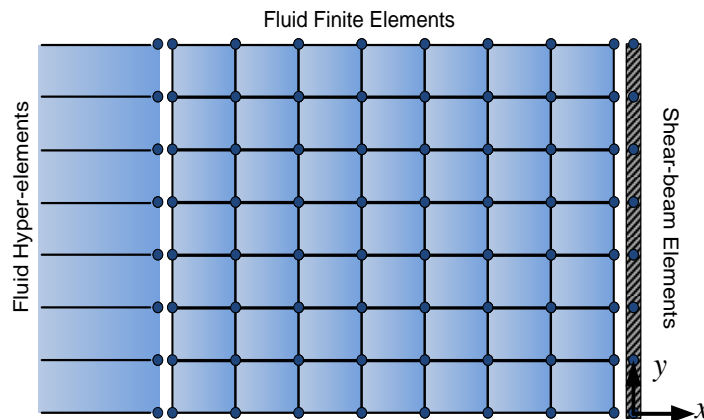


Fig. 3 A schematic finite element mesh for the beam and reservoir

5. Numerical results

Closed-form solution and finite element method for the fluid-structure system were explained in the previous sections. Hereafter, a numerical example is presented and the results of the mentioned methods are compared. The geometrical and mechanical properties of the model are

$$\text{Structure: } \begin{cases} G = 8.33 \times 10^9 & \text{N/m}^2 \\ A = 1 \times 20 & \text{m}^2 \\ \rho = 2500 & \text{Kg/m}^3 \end{cases}, \quad \text{Fluid: } \begin{cases} \rho_F = 1000 & \text{Kg/m}^3 \\ c = 1400 & \text{m/sec.} \\ H = 200 & \text{m} \end{cases}$$

The model consists of a cantilever concrete beam with 200 meters height and a 20×1 rectangular cross section which pure shear deformations are considered. It is assumed that the fluid is compressible water which fills a semi-infinite reservoir of 200 meter height. Moreover, the length of the near field fluid mesh, containing four-node fluid elements, is taken equal to two times of its height in the finite element model.

As for the first response, the frequency response function (FRF) for the acceleration of the beam tip is plotted in Fig. 4. The figure represents the closed-form results from Eq. (33), considering 5, 10 and 20 terms of the series for harmonic horizontal ground acceleration.

It is observed that the three curves are in good agreement within the natural frequencies of 0 to 80 rad/sec. However, the curve with $N=5$ gradually diverges after this frequency due to insufficient number of terms considered in the series. The curves with $N=10$ and $N=20$ are in significant agreement within the shown range of frequencies. This indicates that, as mentioned before, taking only ten terms of the series in Eq. (33) leads to accurate results and the solution can be referred to exact response.

Since the closed-form response for the desired range of frequencies is at hand, the accuracy of the finite element method can be readily verified at this stage. As a result, the acceleration of the beam tip with a mesh of ten elements in height is shown in Fig. 5, in contrast to the closed-form solution.

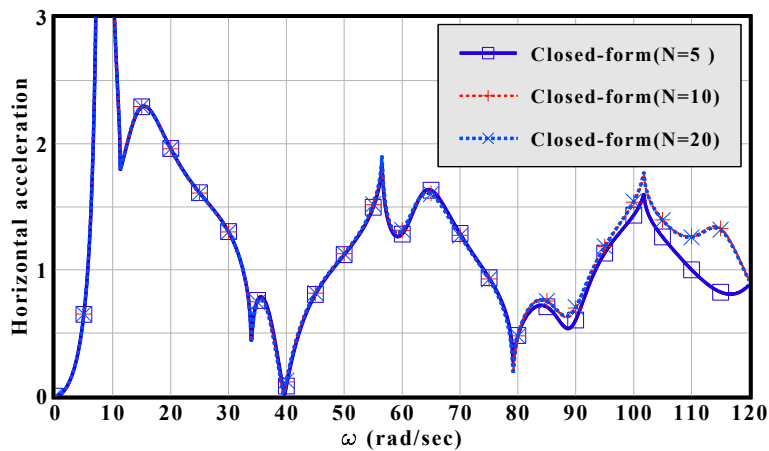


Fig. 4 FRF of the beam tip for different number of series terms in closed-form solution

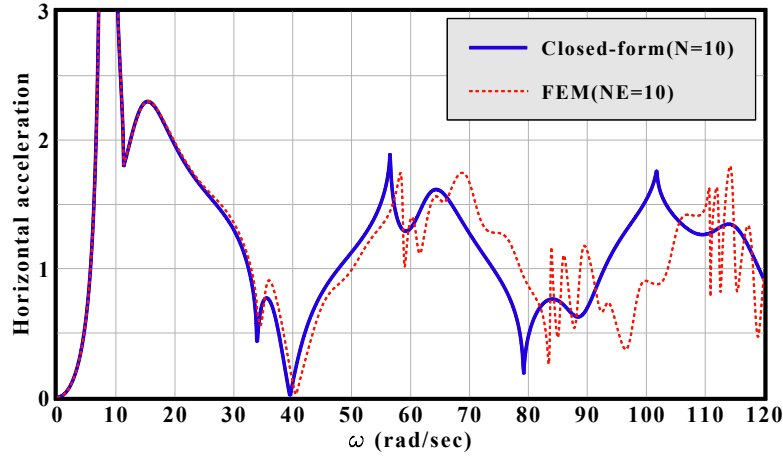


Fig. 5 FEM vs. closed-form acceleration of the beam tip (N=10, NE=10)

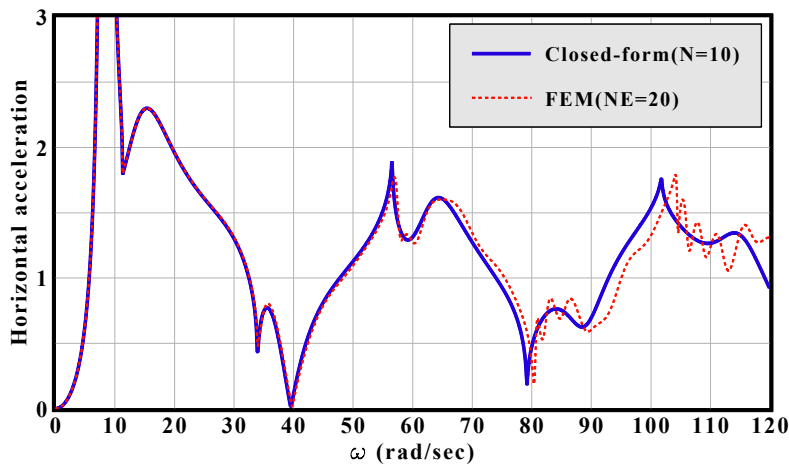


Fig. 6 FEM vs. closed-form acceleration of the beam tip (N=10, NE=20)

It is observed that the finite element response begins to deviate from the closed-form response at natural frequencies of 25 rad/sec. This deviation considerably develops along with frequency increase. To increase accuracy, one may consider mesh refinement in the finite element. This is investigated by doubling the number of the beam and the reservoir elements along the height. Fig. 6 provides a comparison between the refined mesh (NE=20) and the results of the closed-form solution.

The above figure indicates that even with doubling the number of elements, finite element does not provide sufficient accuracy for higher range of frequencies.

Likewise, the frequency response function of the pressure on the beam base ($x = 0, y = 0$) can be determined. This is carried out using finite element (with 10 elements) and the closed-form solution (with 10 terms) as displayed in Fig. 7.

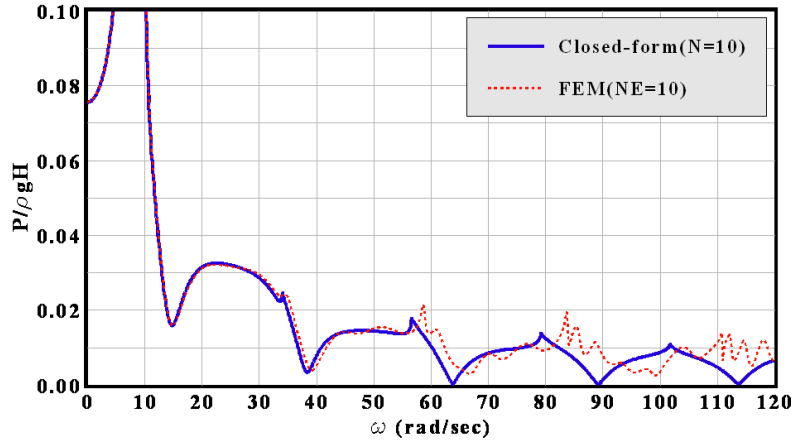


Fig. 7 Pressure frequency response function at base level

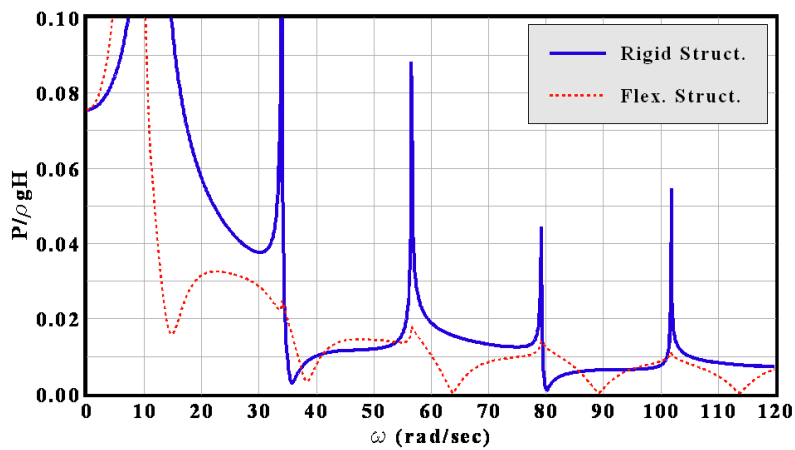


Fig. 8 FRF of pressure at base level for rigid and flexible cases of structure

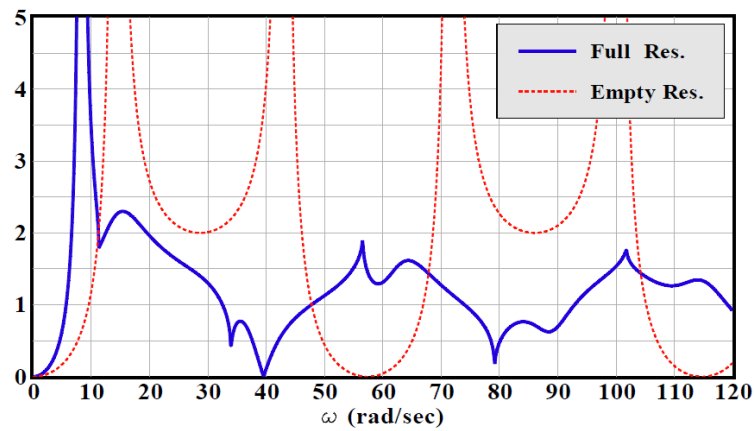


Fig. 9 FRF of beam tip for full and empty reservoir cases

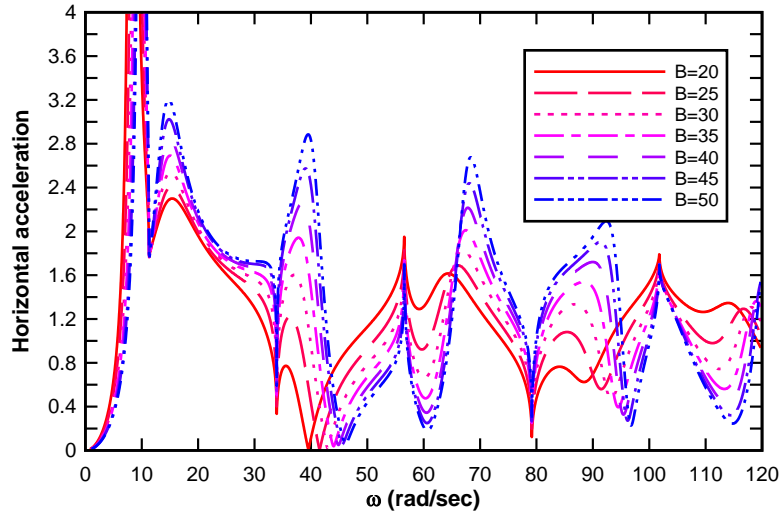


Fig. 10 FRF of acceleration at beam tip for various widths of beam and full reservoir

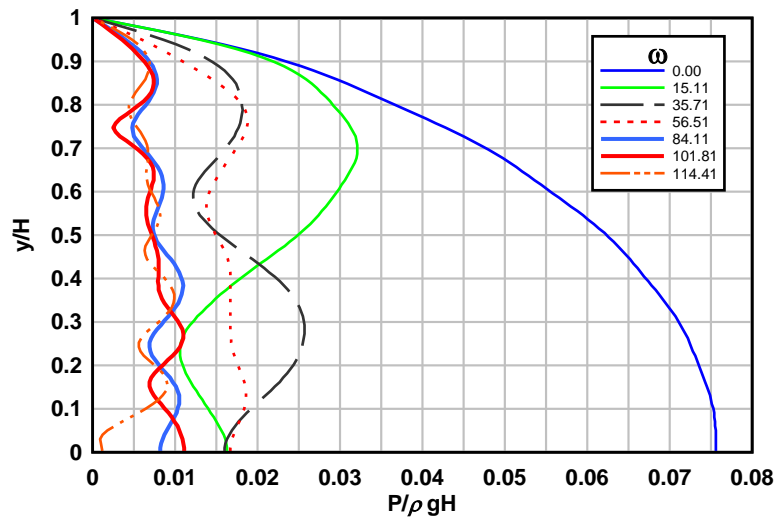


Fig. 11 Normalized hydrodynamic pressure distribution for selected frequencies (closed-form)

The loss of accuracy in finite element results has also been observed in Fig. 7 for higher frequencies. The overall deviations of the curves and their location of occurrence are similar to that of the displacement responses in Fig. 6. Nevertheless, for the pressures, the curves are smoother and the picks display relatively blunt changes.

Moreover, it is convenient to study several special cases. As for the first case, a rigid model of the beam is compared with the flexible beam. In practice, rigidity is achieved by assuming GA to be infinity (a large numeric value). The effect of structure rigidity on pressure frequency response function is shown in Fig. 8.

Interestingly, it is observed that only the first resonance frequency of the system has been

reduced when flexibility is brought into account. In contrast, other resonant frequencies have indicated only a very slight reduction. However, the values of pressures at resonance frequencies of the rigid structure are considerably higher from the values of flexible structure.

Another important case to investigate is an empty reservoir against a full reservoir. This can be achieved by assigning a small value to fluid density. The effect of damping induced by the reservoir can be simply investigated in Fig. 9.

Fig. 9 shows that imposing the interaction effect decreases the value of the first fundamental frequency of the system. Drift of the subsequent resonance frequencies are significant and the coupled system is considerably damped. Moreover, additional resonant frequencies are inserted to the system.

It is of interest to investigate the effect of shear stiffness of the structure on the behavior of the system. Thus, the FRFs of the beam tip for different widths of the cross sections are plotted in Fig. 10. In all cases the depth of the beam is assumed unity. It is observed that the position of resonance frequencies has slightly been affected by variation of the structure width. However, frequencies in all cases are shifted to a greater value.

Furthermore, the normalized hydrodynamic pressure distribution on the beam wet face is shown in Fig. 11. The curves result from closed-form solution and are plotted for several selected excitation frequencies corresponding to the peaks of the frequency response functions.

Although frequency response functions represent the behavior of the system, they are restricted to a single point of the system. In contrast, graphical representation of the pressure contours provides the ability of investigation of the whole system at a certain frequency. This is an effective

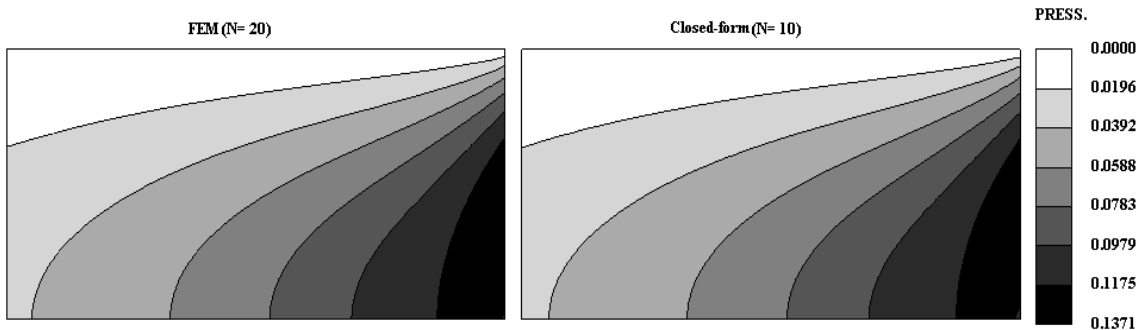


Fig. 12 Pressure distribution of FEM vs. closed-form for $\omega = 10 \text{ rad/sec}$

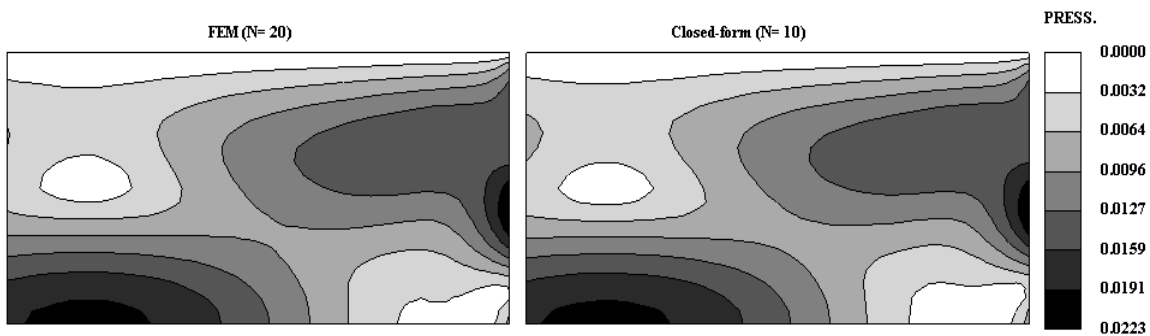


Fig. 13 Pressure distribution of FEM vs. closed-form for $\omega = 40 \text{ rad/sec}$

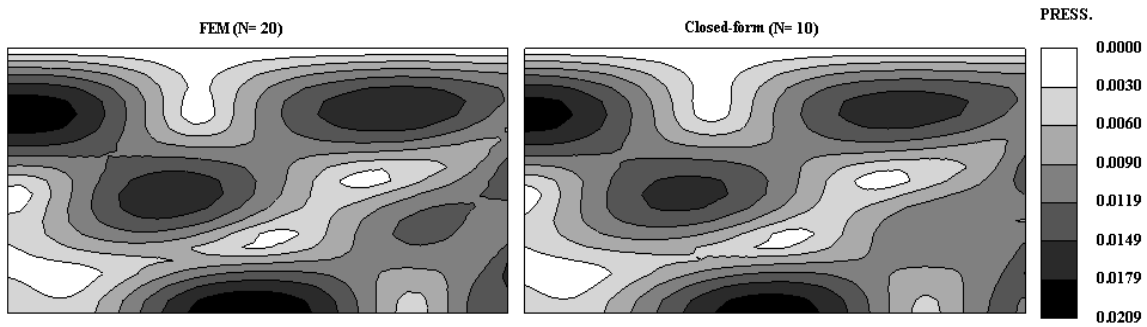


Fig. 14 Pressure distribution of FEM vs. closed-form for $\omega = 60 \text{ rad/sec}$

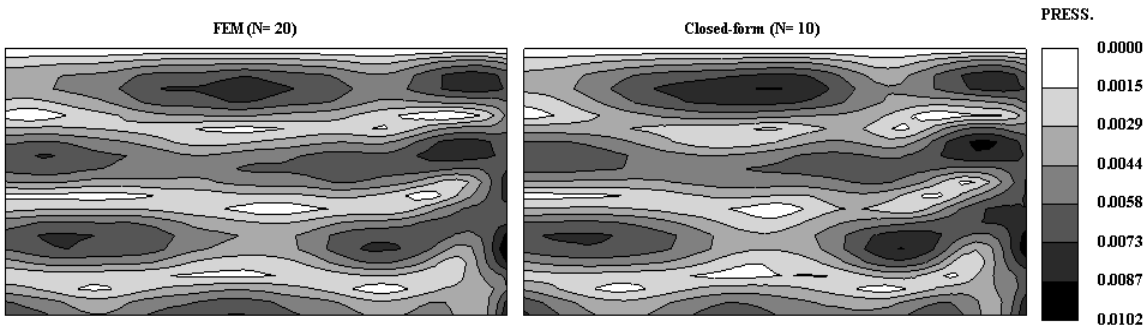


Fig. 15 Pressure distribution of FEM vs. closed-form for $\omega = 100 \text{ rad/sec}$

way to evaluate the accuracy of two analyses since the results contain the whole concerning region and are not restricted to a single point. Accordingly, reservoir pressure contours for closed-form and finite element are shown in Figs. 12-15 for several selected frequencies. The pressure values of the following figures are normalized to hydrostatic pressure in all cases.

Figs. 12-15 indicated that in relatively lower frequencies (within the first and second natural freq.) FEM and closed-form results are in excellent agreement. However, in higher frequencies of excitation, the accuracy of the FEM declines and the corresponding contours deviate from closed-form results (Figs. 14 and 15).

6. Conclusions

A closed-form solution of the fluid-shear beam differential equation was presented in frequency domain under the semi-infinite compressible and irrotational assumptions for the fluid region and horizontal ground excitation. The closed-form solution was used to investigate the accuracy of the conventional finite element method through a numeric example. The displacement of the beam and the pressures of fluid as comparing parameters and special cases such as rigid beam and empty reservoir were investigated in the analysis. Also, sensitivity analysis was carried out on several effective parameters. The following remarks were drawn:

- For low frequencies both methods are in good agreement, while for higher frequencies the finite element responses are not accurate and considerably deviate from closed-form responses.

Moreover, mesh refinement slightly increases the accuracy whereas errors cannot be ignored.

- The computation time for the closed-form solution is significantly less than finite element method. Although one may benefit from efficient storage techniques in finite element method to increase time efficiency, a quite fine mesh is required to achieve the same accuracy.
- For the case of near field earthquakes, where excitation frequencies are high, the closed-form solution provides accurate results, on the contrary with finite element method.
- In many finite element codes, modal analysis is implemented due to efficiency. In such cases, number of participating modes needs to be increased to cover higher frequencies of excitation. Therefore, the efficiency of the method reduces. In contrast, such difficulty is not encountered for closed-form solution, proposed in this study.

References

- Attarnjad, R. and Farsad, A. (2005), "Closed form interaction of dam reservoir system in time domain with variable thickness of dam (in Persian)", *J. Tech. Faculty*, **39**(3), 329-340.
- Avilés, J. and Li, X. (1998), "Analytical-numerical solution for hydrodynamic pressures on dams with sloping face considering compressibility and viscosity of water", *Comput. & Struct.*, **66**(4), 481-488.
- Bejar, L.A.D. (2010), "Time-domain hydrodynamic forces on rigid dams with reservoir bottom absorption of energy", *J. Eng. Mech.*, **136**(10), 1271-1280.
- Bouaanani, N. and Miquel, B. (2010), "A new formulation and error analysis for vibrating dam-reservoir systems with upstream transmitting boundary conditions", *J. Sound Vib.*, **329**(10), 1924-1953.
- Bouaanani, N. and Paultre, P. (2005), "A new boundary condition for energy radiation in covered reservoirs using BEM", *Eng. Anal. Bound. Elem.*, **29**(9), 903-911.
- Bouaanani, N., Paultre, P. and Proulx, J. (2003), "A closed-form formulation for earthquake-induced hydrodynamic pressure on gravity dams", *J. Sound Vib.*, **261**(3), 573-582.
- Bouaanani, N. and Perrault, C. (2010), "Practical formulas for frequency domain analysis of earthquake-induced dam-reservoir interaction", *J. Eng. Mech.*, **136**(1), 107-119.
- Brahtz, H.A. and Heilborn, H. (1933), "Discussion on water pressures on dams during earthquakes", *T. Am. Soc. Civil Eng.*, **98**(2), 452-460.
- Chakrabarti, P. and Chopra, A.K. (1972), "Hydrodynamic pressures and response of gravity dams to vertical earthquake component", *Earthq. Eng. Struct. D.*, **1**(4), 325-335.
- Chopra, A.K. (1967), "Hydrodynamic pressures on dams during earthquake", *J. Engrg. Mech., ASCE*, **93**, 205-223.
- Chopra, A.K. and Chakrabarti, P. (1981), "Earthquake analysis of concrete gravity dams including dam-water-foundation rock interaction", *Earthq. Eng. Struct. D.*, **9**(4), 363-383.
- Chwang, A.T. (1978), "Hydrodynamic pressures on sloping dams during earthquakes. Part 2. Exact theory", *J. Fluid Mech.*, **87**(2), 343-348.
- Ghobarah, A., El-Nady, A. and Aziz, T. (1994), "Simplified dynamic analysis for gravity dams", *J. Struct. Eng.*, **120**(9), 2697-2716.
- Humar, J. and Roufaiel, M. (1983), "Finite element analysis of reservoir vibration", **109**(1), 215-230.
- Kishi, N., Nomachi, S.G., Matsuoka, K.G. and Kida, T. (1987), "Natural frequency of a fill dam by means of two dimensional truncated wedge taking shear and bending moment effects into account", *J. Doboku Gakkai Ronbunshu, Japan Soc. Civil Eng.*, **386**, 43-51.
- Liam Finn, W.D. and Varoglu, E. (1973), "Dynamics of gravity dam-reservoir systems", *Comput. Struct.*, **3**(4), 913-924.
- Lofi, V. (2004), "Frequency domain analysis of concrete gravity dams by decoupled modal approach", *J. Dam Eng.*, **15**(2), 141-165.
- Miquel, B. and Bouaanani, N. (2010), "Simplified evaluation of the vibration period and seismic response of

- gravity dam-water systems”, *Eng. Struct.*, **32**(8), 2488-2502.
- Nasserzare, J., Lei, Y. and Eskandari-Shiri, S. (2000), “Computation of natural frequencies and mode shapes of arch dams as an inverse problem”, *Adv. Eng. Softw.*, **31**(11), 827-836.
- Nath, B. (1971), “Coupled hydrodynamic response of a gravity dam”, *Proceedings of the Institution of Civil Engineers*, **48**(2), 245-257.
- Saini, S.S., Bettess, P. and Zienkiewicz, O.C. (1978), “Coupled hydrodynamic response of concrete gravity dams using finite and infinite elements”, *Earthq. Eng. Struct. D.*, **6**(4), 363-374.
- Sharan, S.K. (1992), “Efficient finite element analysis of hydrodynamic pressure on dams”, *Comput. Struct.*, **42**(5), 713-723.
- Tsai, C.S. and Lee, G.C. (1990), “Method for transient analysis of three-dimensional dam-reservoir interactions”, *J. Eng. Mech.*, **116**(10), 2151-2172.
- Tsai, C.S. (1992), “Semi-analytical solution for hydrodynamic pressures on dams with arbitrary upstream face considering water compressibility”, *Comput. Struct.*, **42**(4), 497-502.
- Westergaard, H.M. (1933), “Water pressures on dams during earthquakes”, *T. Am. Soc. Civil Eng.*, **98**(2), 471-472.

Appendix

The finite element discretisation of Eq. (1) results in the following matrices

$$\mathbf{H} = \frac{1}{6} \begin{pmatrix} 4 & -1 & -2 & -1 \\ -1 & 4 & -1 & -2 \\ -2 & -1 & 4 & -1 \\ -1 & -2 & -1 & 4 \end{pmatrix}, \mathbf{G} = \frac{L^2}{36} \begin{pmatrix} 4 & 2 & 1 & 2 \\ 2 & 4 & 2 & 1 \\ 1 & 2 & 4 & 2 \\ 2 & 1 & 2 & 4 \end{pmatrix} \quad (\text{A.1})$$

where, \mathbf{H}, \mathbf{G} are stiffness and mass matrices of a typical square element in near-field reservoir. Hyperelement matrix regarding the far-field reservoir are given by

$$\mathbf{H}_h = \mathbf{A}\mathbf{X}\mathbf{K}\mathbf{X}\mathbf{A} \quad (\text{A.2})$$

Where \mathbf{X} contains the eigenvectors of the following eigen-problem

$$\mathbf{C}\mathbf{X}_i = \lambda_i \mathbf{A}\mathbf{X}_i \quad (\text{A.3})$$

\mathbf{A}, \mathbf{C} are defined for each layer of elements of the height h by

$$\mathbf{A} = \frac{h}{6} \begin{pmatrix} 2 & 1 \\ 1 & 2 \end{pmatrix}, \mathbf{C} = \frac{1}{h} \begin{pmatrix} +1 & -1 \\ -1 & +1 \end{pmatrix} \quad (\text{A.4})$$

Also, \mathbf{K} is a diagonal matrix, defined by

$$\mathbf{K} = \text{diag} \left[\sqrt{\lambda_i^2 - \left(\frac{\omega}{c} \right)^2} \right], i = 1, \dots, n \quad (\text{A.5})$$